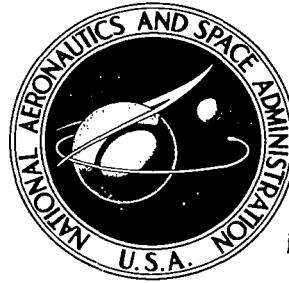


NASA TECHNICAL NOTE



NASA TN D-4796

0.1

NASA TN D-4796

LOAN COPY: R
AFWL (W
KIRTLAND AFI

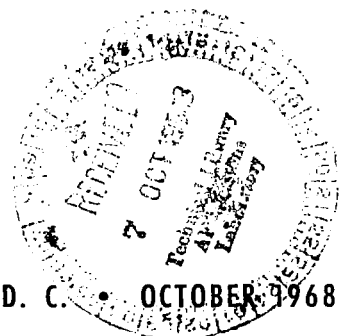


EFFECT OF SHAPE CHANGES ON THE
AERODYNAMIC CHARACTERISTICS OF A
TWISTED AND CAMBERED ARROW WING
AT MACH NUMBER 2.03

by Emma Jean Landrum and Barrett L. Shrout

Langley Research Center

Langley Station, Hampton, Va.



NATIONAL AERONAUTICS AND SPACE ADMINISTRATION • WASHINGTON, D. C. • OCTOBER 1968



EFFECT OF SHAPE CHANGES ON THE AERODYNAMIC CHARACTERISTICS
OF A TWISTED AND CAMBERED ARROW WING AT MACH NUMBER 2.03

By Emma Jean Landrum and Barrett L. Shrout

Langley Research Center
Langley Station, Hampton, Va.

NATIONAL AERONAUTICS AND SPACE ADMINISTRATION

For sale by the Clearinghouse for Federal Scientific and Technical Information
Springfield, Virginia 22151 - CFSTI price \$3.00

EFFECT OF SHAPE CHANGES ON THE AERODYNAMIC CHARACTERISTICS OF A TWISTED AND CAMBERED ARROW WING AT MACH NUMBER 2.03

By Emma Jean Landrum and Barrett L. ShROUT
Langley Research Center

SUMMARY

The investigation was conducted in the Langley 4- by 4-foot supersonic pressure tunnel at a Reynolds number, based on wing mean geometric chord, of 4.4×10^6 . The basic wing had a design lift coefficient of 0.08, a leading-edge sweep angle of 70° , and an aspect ratio of 2.24. The effects of shearing the inboard region, reducing the twist of the inboard region, and reflexing the aft portion of the wing were examined.

When higher values of zero-lift pitching moment are required for a given wing the most promising modification of those examined was trailing-edge reflex. However, when extensive changes are permitted, a redesign of the entire camber surface would undoubtedly be the most desirable process.

INTRODUCTION

A theoretical method for the design of twisted and cambered wings of arbitrary planform has been presented in reference 1. This method, based on linear theory, assumes that the wing is essentially in a plane, that is, any displacement in the vertical direction may be neglected. Considerable interest has been shown recently in determining experimentally the validity of this assumption and also in determining the effects of modifications to theoretically optimum or near-optimum wings in order to obtain more practical shapes in the root regions or to obtain positive zero-lift pitching-moment increments.

The purpose of this investigation was to examine the effects of modifying a twisted and cambered wing whose basic aerodynamic characteristics are well established. This wing is the 70° sweepback, 0.08 design-lift-coefficient wing reported in references 2 and 3. Four wings were tested in addition to the basic wing which was retested to insure the consistency of the data. One wing had the inboard stations lowered with respect to the reference plane so that a straight leading edge was obtained. Another wing had the inboard stations raised with respect to the reference plane so that the camber surface was flat across the top at 65 percent of the overall length of the wing. These two wings with the basic wing provide a series of wings to examine the effects of shearing the

inboard wing sections in the vertical direction while maintaining the streamwise camber lines unchanged. Modifications of the basic camber surface in the streamwise direction were employed in the design of two other wings. One of these had a reduced angle of twist in the inboard sections, a type of modification which might be required to obtain more practical shapes for landing gear or other component integration. The trailing edge of the other wing was modified to follow a $3/2$ power curve from root to tip resulting in considerable reflexing of the wing near the root. This reflexing should provide an appreciable positive zero-lift pitching-moment increment.

Tests were conducted in the Langley 4- by 4-foot supersonic pressure tunnel at a Mach number of 2.03 and a Reynolds number, based on mean geometric chord, of 4.4×10^6 .

SYMBOLS

b	wing span
c	chord
c_r	root chord
\bar{c}	wing mean geometric chord
C_D	drag coefficient, Drag/qS
C_L	lift coefficient, Lift/qS
C_{L_α}	lift-curve slope, $\partial C_L / \partial \alpha$, per degree
C_m	pitching-moment coefficient about $\bar{c}/4$, $\text{Pitching moment}/qS\bar{c}$
l	overall length of wing
L/D	lift-drag ratio, C_L/C_D
M	free-stream Mach number
q	free-stream dynamic pressure
S	wing area

x,y,z	Cartesian coordinate system with origin at wing apex, X-axis streamwise
x'	distance rearward from leading edge
x^*	distance from apex to location at which camber surface is flat in lateral direction
z_c	camber surface ordinate, positive up (measured from reference plane)
α	angle of attack, degrees

Subscripts:

max	maximum
trim	trim conditions
o	zero lift

MODELS AND INSTRUMENTATION

A sketch of the wing planform is shown in figure 1. The basic wing, designated wing 1 in this report, has a design lift coefficient of 0.08 and is geometrically identical to wing 2 of reference 2. The wing has a 70° swept leading edge and aspect ratio of 2.24. The thickness distribution of the wing is formed by a 3-percent-thick circular-arc airfoil section in the streamwise direction. This thickness was added symmetrically to the mean-camber ordinates.

Nondimensional camber surface ordinates for the five wings are given in table I. For wing 2, the inboard stations are lowered with respect to the reference plane so that a straight leading edge is obtained. The ordinates outboard of station $\frac{y}{b/2} = 0.30$ are the same as wing 1. The inboard stations of wing 3 have been raised with respect to the reference plane so that the camber surface is flat across the top at 65 percent of the overall length of the wing. Outboard of station $\frac{y}{b/2} = 0.60$ wing 3 is the same as wing 1.

Wing 4 has the angle of twist for the inboard stations reduced. From station $\frac{y}{b/2} = 0.30$ outboard the ordinates are the same as wing 1. The root-chord trailing edge of wing 5 was raised an amount equivalent to reducing the twist of the root chord to 0.735 that of wing 1. This increment was decreased to zero at the tip by a $3/2$ power

variation along the span. The forepart of the wing is the same as wing 1. The upper surface of each streamwise section is a straight line through the corresponding trailing-edge point and tangent to the forepart of the wing aft of the 40-percent-chord station. The reflexing of wing 5 is similar to the type of reflex used for the configuration of reference 4.

The wings were attached to a four-component strain-gage balance housed within a horizontal splitter plate (fig. 2). The plate was supported by a permanent sting mounting system of the Langley 4- by 4-foot supersonic pressure tunnel. Changes in angle of attack were made by moving the wing and plate as a single unit. A very small gap between the plate and the wing prevented model-to-plate fouling.

TESTS AND ACCURACY

The tests were conducted in the Langley 4- by 4-foot supersonic pressure tunnel at a Mach number of 2.03 and a Reynolds number based on \bar{c} of 4.4×10^6 . Transition strips of No. 60 carborundum grains, 0.318 cm wide, were placed 1.01 cm streamwise back from the leading edge of the wings. After the force tests on some of the wings, drag data were taken through the Reynolds number range to insure that the test Reynolds number was well above the Reynolds number range for transition to fully turbulent flow.

Angle of attack was measured optically through the use of prisms recessed in the wing surfaces.

The Mach number and aerodynamic coefficients are estimated to be accurate within the following limits:

M	±0.02
C_D	±0.0003
C_L	±0.0030
C_m	±0.0010

Although there may be some grit drag present in the data, the experimental data have not been corrected for grit drag since the amount is believed to be within the accuracy of the data.

RESULTS AND DISCUSSION

Basic longitudinal aerodynamic characteristics for the five wings are presented in figure 3. All the wings have essentially the same $C_{L\alpha}$ and $\partial C_m / \partial C_L$. Lift-drag ratios are compared in figure 4. The basic wing (wing 1) has the highest $(L/D)_{\max}$. The various parameters are summarized in the following table:

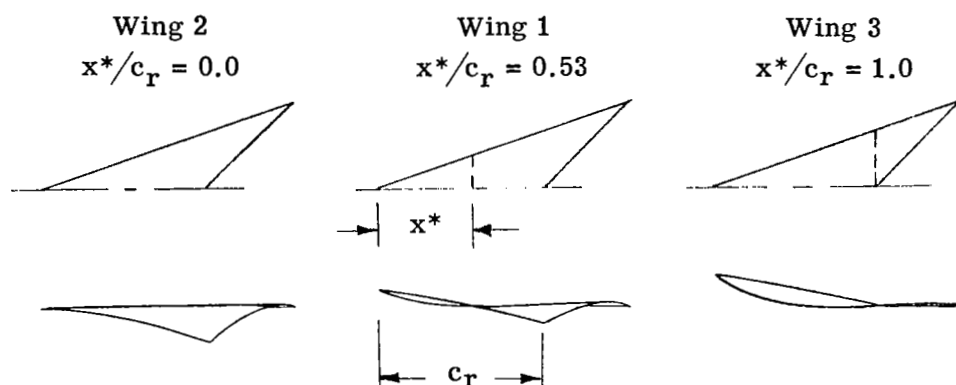
Wing	$C_{L\alpha}$	$C_{m,o}$	$\frac{\partial C_m}{\partial C_L}$	$\frac{\Delta C_D}{\Delta C_L^2}$	$(L/D)_{\max}$
1	0.0309	0.0065	-0.295	0.394	8.80
2	.0314	.0054	-.300	.394	8.25
3	.0304	.0098	-.290	.410	8.30
4	.0308	.0022	-.296	.396	8.60
5	.0308	.0162	-.295	.439	8.10

The data points for $\Delta C_D / \Delta C_L^2$ were obtained from the linear portion of a plot of C_D as a function of C_L^2 for each wing.

Reducing the twist of the inboard region (wing 4) significantly decreases $C_{m,o}$ while changing $\Delta C_D / \Delta C_L^2$ very little. Reflexing the aft region (wing 5) provided large increases in $C_{m,o}$ and, correspondingly, a considerable increase in $\Delta C_D / \Delta C_L^2$.

Effects of Shear

The effects of shear are shown in figure 5. The abscissa is the distance from the apex to the location at which the camber surface is flat in the lateral direction normalized by the root chord. (See the following sketch.)



It can be seen that the result of shearing the root region is substantial changes in $(L/D)_{\max}$ and in $C_{m,o}$. The theoretical method of reference 1 does not take into account the changes in the perturbation paths due to vertical displacement within the camber plane and, as a consequence, predicts constant values for the aerodynamic parameters regardless of shear. Where large displacements in the vertical direction are required, the theoretical method should be used with some caution.

Some further insight into the physical phenomena which occur as a result of shear may be obtained by examining the vertical displacement of the leading and trailing edges (shown in fig. 6) since the major portion of the vertical displacement of the camber

surface is within the vertical limits of the leading and trailing edges (table I). The development of upwash along the leading edge is affected by the vertical displacement of the apex so that, as displacement increases, a decrease in upwash and a loss in lift occurs over the outboard portions of the wing. This results in a higher pitching-moment coefficient for a given lift as can be seen from the data.

Trim Effects

One of the critical problems of the designers of supersonic aircraft is that of trimming the aircraft. If, through moderate reshaping of large portions of the basic camber plane, an appreciable zero-lift pitching-moment increment can be made available, without significantly degrading drag due to lift, the trim problem would be greatly alleviated. In order to examine the effects of trim drag, incremental data for controls on an arrow wing from reference 5 were used with the basic data shown in figure 3. It should be pointed out that the control data used is for a flat wing. Since all the wings of this investigation are the same in the tip region, although twisted and cambered, a tip control using flat-wing control data should provide a qualitative insight into trim effects.

Using the correlations of reference 5, data for a control with hinge line perpendicular to the free-stream direction and with a control-to-wing area ratio of 0.2 were superimposed on the data for each wing. The results are presented in figure 7. Included also are data for the flat wing of reference 5. Reflexing the aft portion of the wing (wing 5) is shown to provide much higher $(L/D)_{\text{trim,max}}$ at the higher stability levels. Wing 3 (root sheared up) also shows a gain in trim efficiency at the higher stability levels. The substantially larger gains shown for wing 5 over wing 3 can be attributed to the fact that the additional loss in $(L/D)_{\text{max}}$ for the reflexed wing is more than offset by the additional increase in $C_{m,0}$.

CONCLUDING REMARKS

The results of this investigation at a Mach number of 2.03 into the effects of modifying a twisted and cambered wing indicate that care must be taken before making modifications so that the benefits obtained from optimization are not lost. The basic wing of this investigation is itself a carefully modified wing since construction techniques necessitated local tailoring in the root region of the optimized theoretical wing.

Use of the theoretical method of NASA Technical Note D-2341 to design or evaluate wings which have large displacements in the vertical direction will require careful consideration of all the factors involved. Insofar as the actual data are concerned a primary effect will be in the accuracy of the zero-lift pitching moment.

When higher values of zero-lift pitching moment are required for a given wing the most promising modification of those examined was trailing-edge reflex. Even though other types of modifications, shearing the root region or reducing the twist of the root region, do not appear as promising from an aerodynamic viewpoint a knowledge of their effects is necessary in assessing the characteristics of a complete aircraft configuration. When extensive changes are permitted, however, a redesign of the entire camber surface would undoubtedly be the most desirable process.

Langley Research Center,
National Aeronautics and Space Administration,
Langley Station, Hampton, Va., June 10, 1968,
126-13-02-37-23.

REFERENCES

1. Carlson, Harry W.; and Middleton, Wilbur D.: A Numerical Method for the Design of Camber Surfaces of Supersonic Wings With Arbitrary Planforms. NASA TN D-2341, 1964.
2. Carlson, Harry W.: Aerodynamic Characteristics at Mach Number 2.05 of a Series of Highly Swept Arrow Wings Employing Various Degrees of Twist and Camber. NASA TM X-332, 1960.
3. Carlson, Harry W.: Pressure Distributions at Mach Number 2.05 on a Series of Highly Swept Arrow Wings Employing Various Degrees of Twist and Camber. NASA TN D-1264, 1962.
4. Robins, A. Warner; Spearman, M. Leroy; and Harris, Roy V., Jr.: Aerodynamic Characteristics at Mach Numbers of 2.30, 2.60, and 2.96 of a Supersonic Transport Model With a Blended Wing-Body, Variable-Sweep Auxiliary Wing Panels, Outboard Tail Surfaces, and a Design Mach Number of 2.6. NASA TM X-815, 1963.
5. Landrum, Emma Jean: Effect of Skewed Wing-Tip Controls on a Highly Swept Arrow Wing at Mach Number 2.03. NASA TN D-1867, 1964.

TABLE I.- WING CAMBER SURFACE ORDINATES, $z_c/lC_{L,design}$

$$[C_{L,design} = 0.08]$$

x'/c	$z_c/lC_{L,design}$ for $\frac{y}{b/2}$ of -										
	0	0.10	0.20	0.30	0.40	0.50	0.60	0.70	0.80	0.90	1.00
Wing 1											
0	0.4000	0.1566	0.0550	0.0170	0.0226	0.0280	0.0326	0.0380	0.0433	0.0480	0.0533
.025	.3866	.1593	.0580	.0223	.0300	.0320	.0366	.0420	.0476	.0496	
.050	.3700	.1593	.0620	.0256	.0340	.0350	.0400	.0446	.0486	.0506	
.100	.3366	.1533	.0620	.0290	.0370	.0400	.0453	.0500	.0533	.0533	
.200	.2733	.1233	.0480	.0230	.0367	.0456	.0520	.0566	.0590	.0573	
.300	.2020	.0870	.0270	.0110	.0313	.0450	.0540	.0600	.0640	.0610	
.400	.1300	.0430	0	-.0040	.0223	.0400	.0520	.0620	.0666	.0646	
.500	.0580	-.0040	-.0280	-.0220	.0100	.0333	.0500	.0616	.0680	.0670	
.600	-.0170	-.0533	-.0590	-.0433	-.0037	.0250	.0460	.0600	.0686	.0690	
.700	-.0980	-.1000	-.0906	-.0650	-.0197	.0150	.0373	.0570	.0686	.0710	
.800	-.1800	-.1433	-.1240	-.0883	-.0370	.0040	.0316	.0540	.0680	.0726	
.900	-.2640	-.1876	-.1560	-.1133	-.0550	-.0080	.0260	.0500	.0666	.0736	
1.000	-.3466	-.2296	-.1850	-.1350	-.0733	-.0213	.0180	.0453	.0653	.0746	
Wing 2											
0	0	0.0045	0.0121	0.0170	0.0226	0.0280	0.0326	0.0380	0.0433	0.0480	0.0533
.025	-.0134	.0072	.0151	.0223	.0300	.0320	.0366	.0420	.0476	.0496	
.050	-.0300	.0072	.0191	.0256	.0340	.0350	.0400	.0446	.0486	.0506	
.100	-.0634	.0012	.0191	.0290	.0370	.0400	.0453	.0500	.0533	.0533	
.200	-.1267	-.0288	.0051	.0230	.0367	.0456	.0520	.0566	.0590	.0573	
.300	-.1980	-.0651	-.0159	.0110	.0313	.0450	.0540	.0600	.0640	.0610	
.400	-.2700	-.1091	-.0429	-.0040	.0223	.0400	.0520	.0620	.0666	.0646	
.500	-.3420	-.1561	-.0709	-.0220	.0100	.0333	.0500	.0616	.0680	.0670	
.600	-.4170	-.2054	-.1019	-.0433	-.0037	.0250	.0460	.0600	.0686	.0690	
.700	-.4980	-.2521	-.1335	-.0650	-.0197	.0150	.0373	.0570	.0686	.0710	
.800	-.5800	-.2954	-.1669	-.0883	-.0370	.0040	.0316	.0540	.0680	.0726	
.900	-.6640	-.3397	-.1989	-.1133	-.0550	-.0080	.0260	.0500	.0666	.0736	
1.000	-.7466	-.3817	-.2279	-.1350	-.0733	-.0213	.0180	.0453	.0653	.0746	
Wing 3											
0	0.8029	0.4137	0.2508	0.1512	0.0855	0.0438	0.0326	0.0380	0.0433	0.0480	0.0533
.025	.7895	.4164	.2538	.1565	.0929	.0478	.0366	.0420	.0476	.0496	
.050	.7727	.4164	.2578	.1598	.0969	.0508	.0400	.0446	.0486	.0506	
.100	.7395	.4104	.2578	.1632	.0999	.0558	.0453	.0500	.0533	.0533	
.200	.6762	.3804	.2438	.1572	.0996	.0614	.0520	.0566	.0590	.0573	
.300	.6049	.3441	.2228	.1452	.0942	.0608	.0540	.0600	.0640	.0610	
.400	.5329	.3001	.1958	.1302	.0852	.0558	.0520	.0620	.0666	.0646	
.500	.4609	.2531	.1678	.1122	.0729	.0491	.0500	.0616	.0680	.0670	
.600	.3859	.2038	.1368	.0909	.0592	.0408	.0460	.0600	.0686	.0690	
.700	.3049	.1571	.1052	.0692	.0432	.0308	.0373	.0570	.0686	.0710	
.800	.2229	.1138	.0718	.0459	.0259	.0198	.0316	.0540	.0680	.0726	
.900	.1389	.0695	.0398	.0209	.0079	.0078	.0260	.0500	.0666	.0736	
1.000	.0563	.0275	.0108	-.0008	-.0104	-.0055	.0180	.0453	.0653	.0746	

TABLE I.- WING CAMBER SURFACE ORDINATES, $z_c/lC_{L,design}$ - Concluded

x'/c	$z_c/lC_{L,design}$ for $\frac{y}{b/2}$ of -										
	0	0.10	0.20	0.30	0.40	0.50	0.60	0.70	0.80	0.90	1.00
Wing 4											
0	0.1996	0.1213	0.0513	0.0170	0.0226	0.0280	0.0326	0.0380	0.0433	0.0480	0.0533
.025	.1933	.1258	.0542	.0223	.0300	.0320	.0366	.0420	.0476	.0496	
.050	.1879	.1279	.0588	.0256	.0340	.0350	.0400	.0446	.0486	.0506	
.100	.1733	.1263	.0596	.0290	.0370	.0400	.0453	.0500	.0533	.0533	
.200	.1471	.1046	.0467	.0230	.0367	.0456	.0520	.0566	.0590	.0573	
.300	.1133	.0767	.0271	.0110	.0313	.0450	.0540	.0600	.0640	.0610	
.400	.0783	.0408	.0017	-.0040	.0223	.0400	.0520	.0620	.0666	.0646	
.500	.0438	.0017	-.0250	-.0220	.0100	.0333	.0500	.0616	.0680	.0670	
.600	.0058	-.0392	-.0550	-.0433	-.0037	.0250	.0460	.0600	.0686	.0690	
.700	-.0379	-.0775	-.0854	-.0650	-.0197	.0150	.0373	.0570	.0686	.0710	
.800	-.0825	-.1125	-.1171	-.0883	-.0370	.0040	.0316	.0540	.0680	.0726	
.900	-.1296	-.1483	-.1475	-.1133	-.0550	-.0080	.0260	.0500	.0666	.0736	
1.000	-.1746	-.1821	-.1754	-.1350	-.0733	-.0213	.0180	.0453	.0653	.0746	
Wing 5											
0	0.4000	0.1566	0.0550	0.0170	0.0226	0.0280	0.0326	0.0380	0.0433	0.0480	0.0533
.025	.3866	.1593	.0580	.0223	.0300	.0320	.0366	.0420	.0476	.0496	
.050	.3700	.1593	.0620	.0256	.0340	.0350	.0400	.0446	.0486	.0506	
.100	.3366	.1533	.0620	.0290	.0370	.0400	.0453	.0500	.0533	.0533	
.200	.2733	.1233	.0480	.0230	.0367	.0456	.0520	.0566	.0590	.0573	
.300	.2020	.0870	.0270	.0110	.0313	.0450	.0540	.0600	.0640	.0610	
.400	.1300	.0430	0	-.0040	.0223	.0400	.0520	.0620	.0666	.0646	
.500	.0588	.0038	-.0267	-.0238	.0100	.0333	.0500	.0616	.0680	.0670	
.600	-.0008	-.0271	-.0458	-.0367	.0004	.0250	.0460	.0600	.0686	.0690	
.700	-.0538	-.0488	-.0571	-.0425	-.0038	.0233	.0454	.0604	.0686	.0710	
.800	-.0958	-.0617	-.0604	-.0417	-.0025	.0271	.0488	.0633	.0713	.0733	
.900	-.1275	-.0658	-.0563	-.0338	.0050	.0354	.0563	.0696	.0763	.0767	
1.000	-.1496	-.0613	-.0438	-.0196	.0183	.0483	.0675	.0779	.0829	.0808	

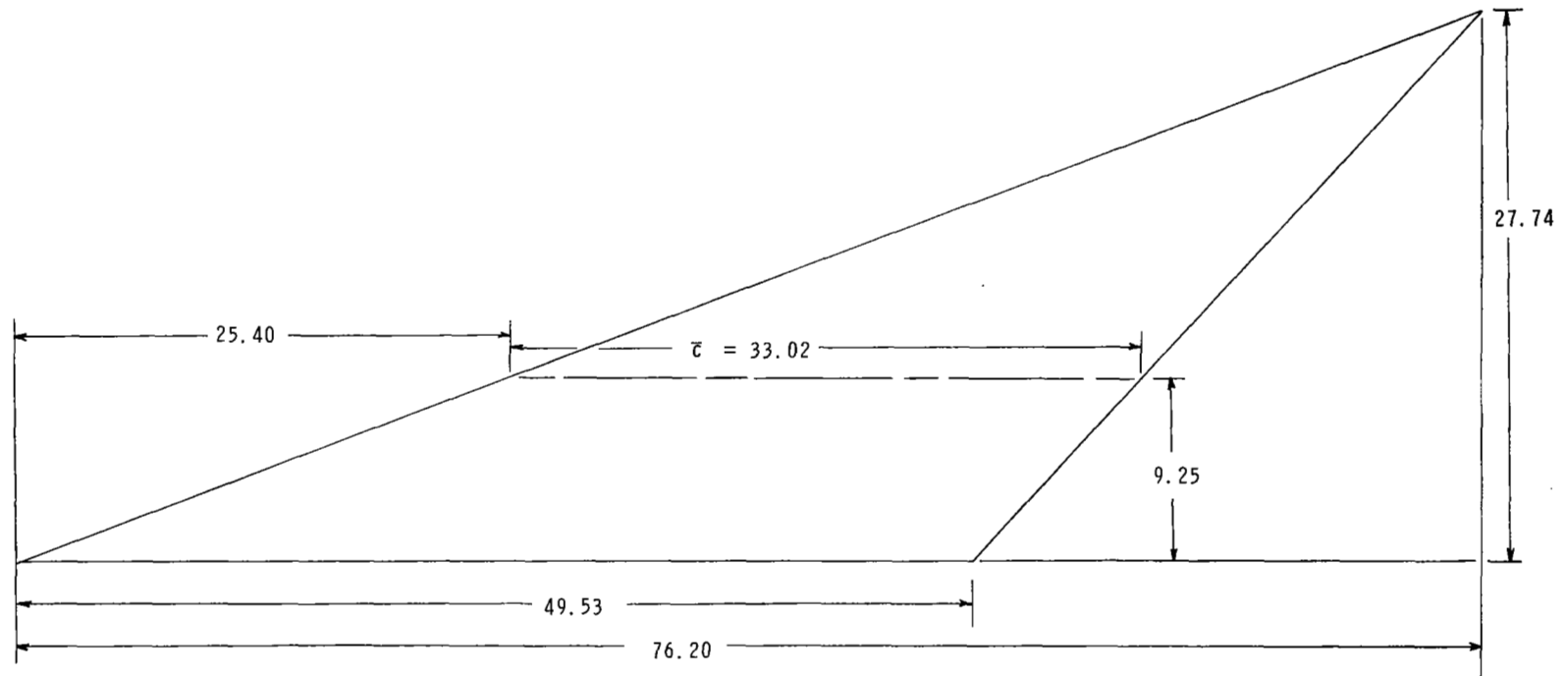
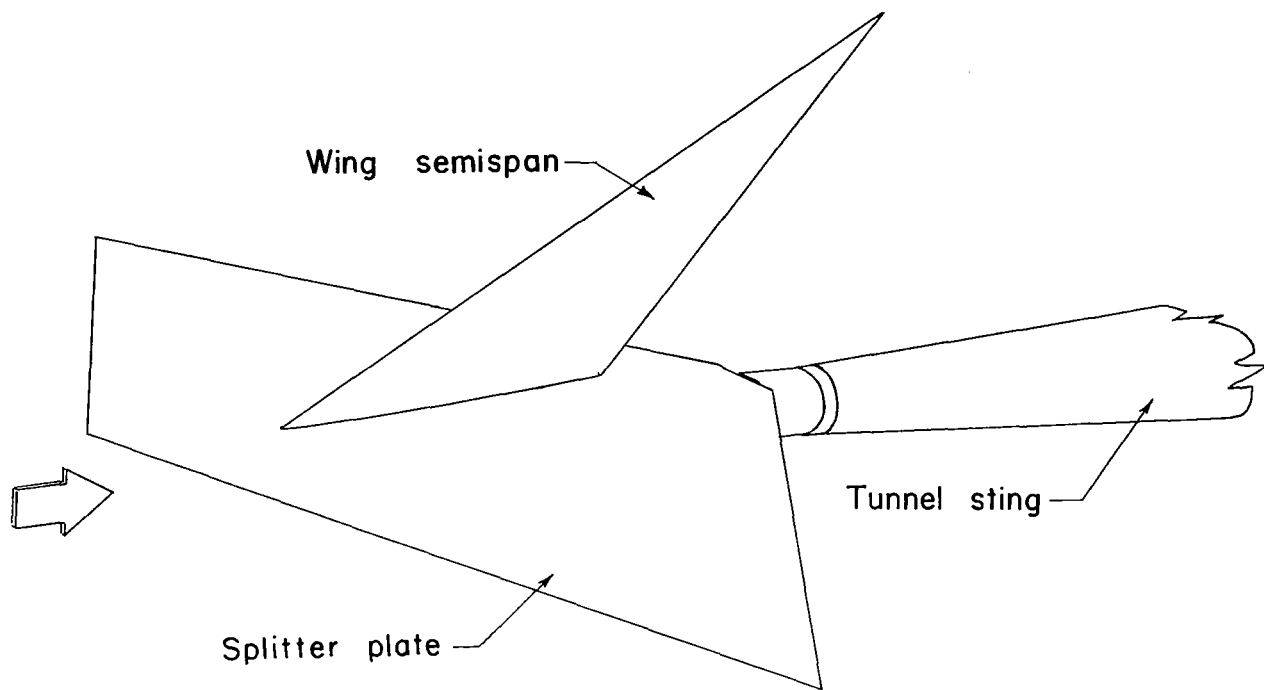
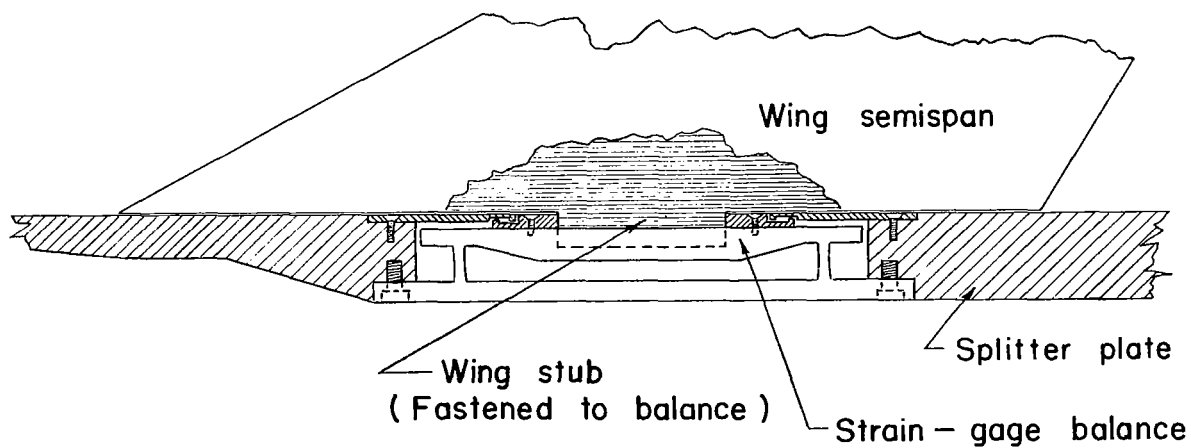


Figure 1.- Sketch of model. All dimensions are in centimeters.

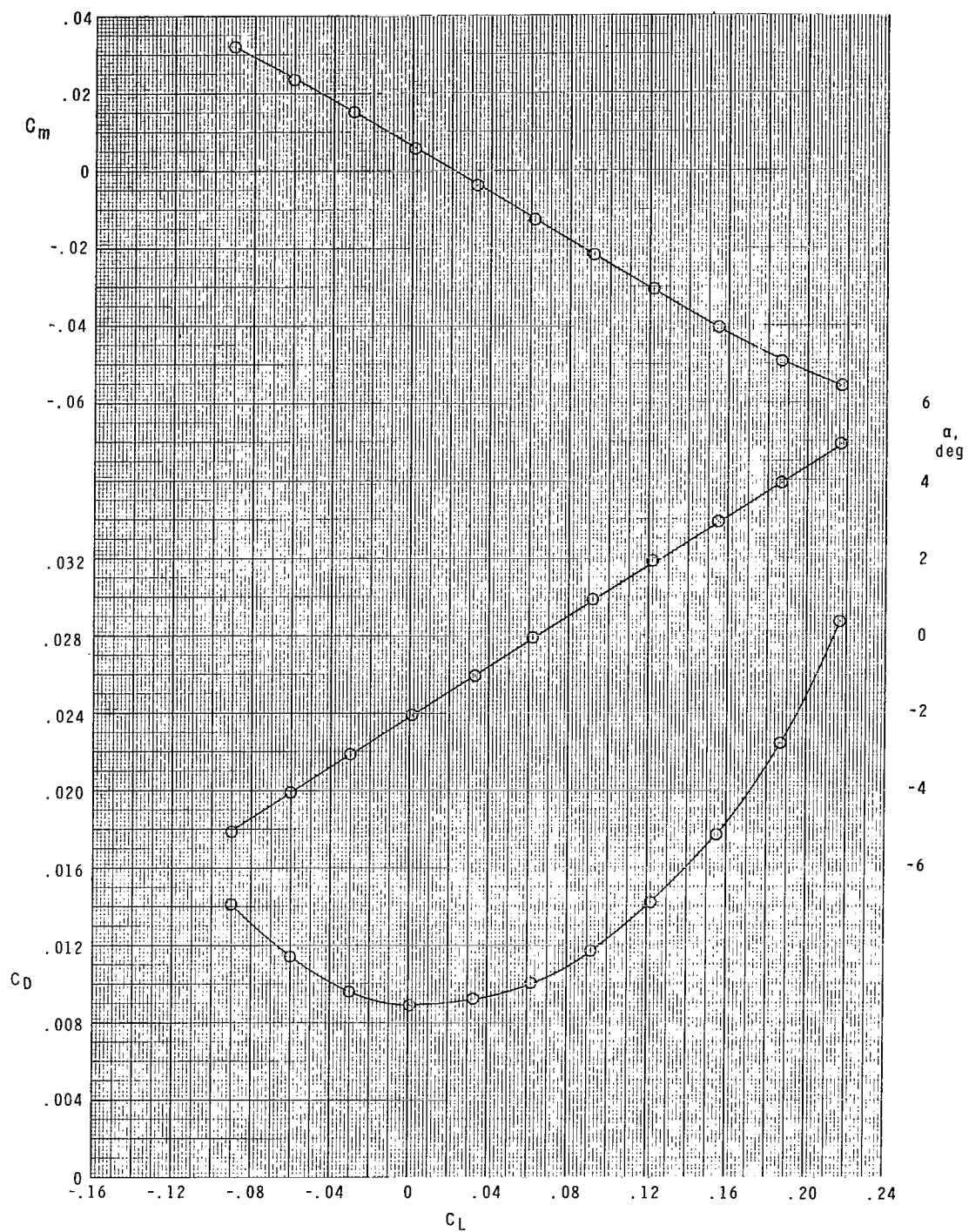


(a) Test rig in tunnel. Upper surface of splitter plate is parallel to tunnel flow.



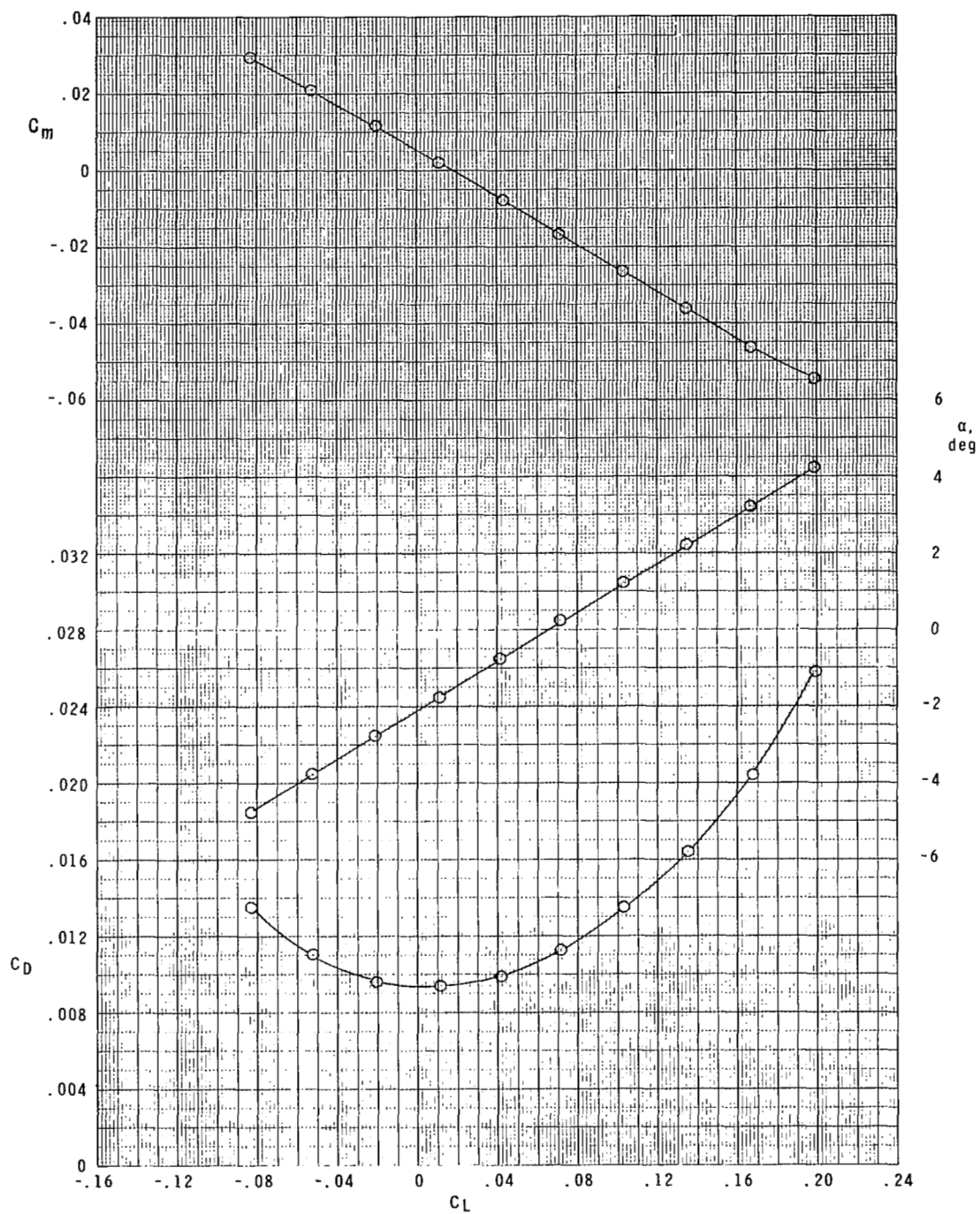
(b) Plate-balance-model details.

Figure 2.- Sketch of test setup.



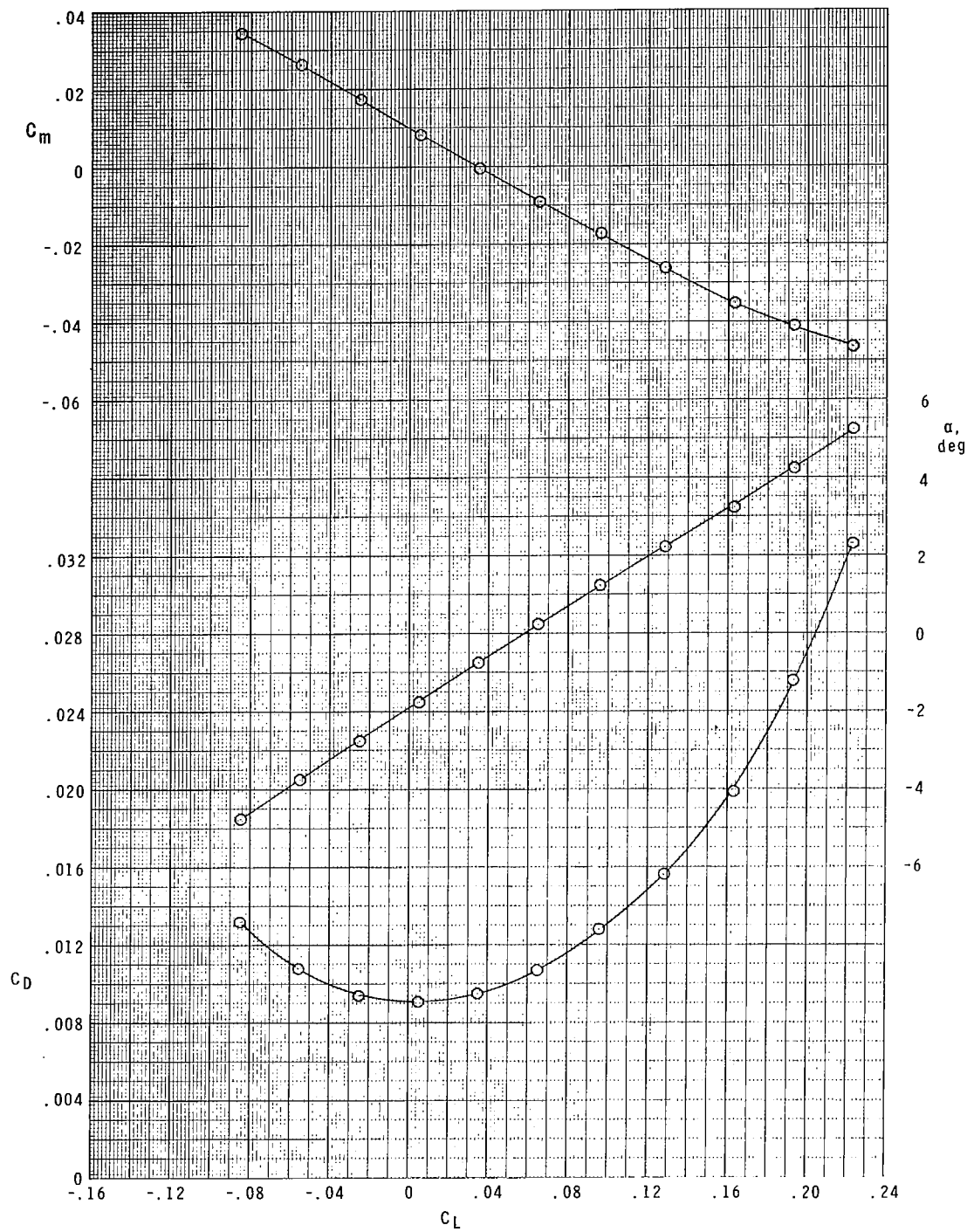
(a) Wing 1.

Figure 3.- Longitudinal aerodynamic characteristics.



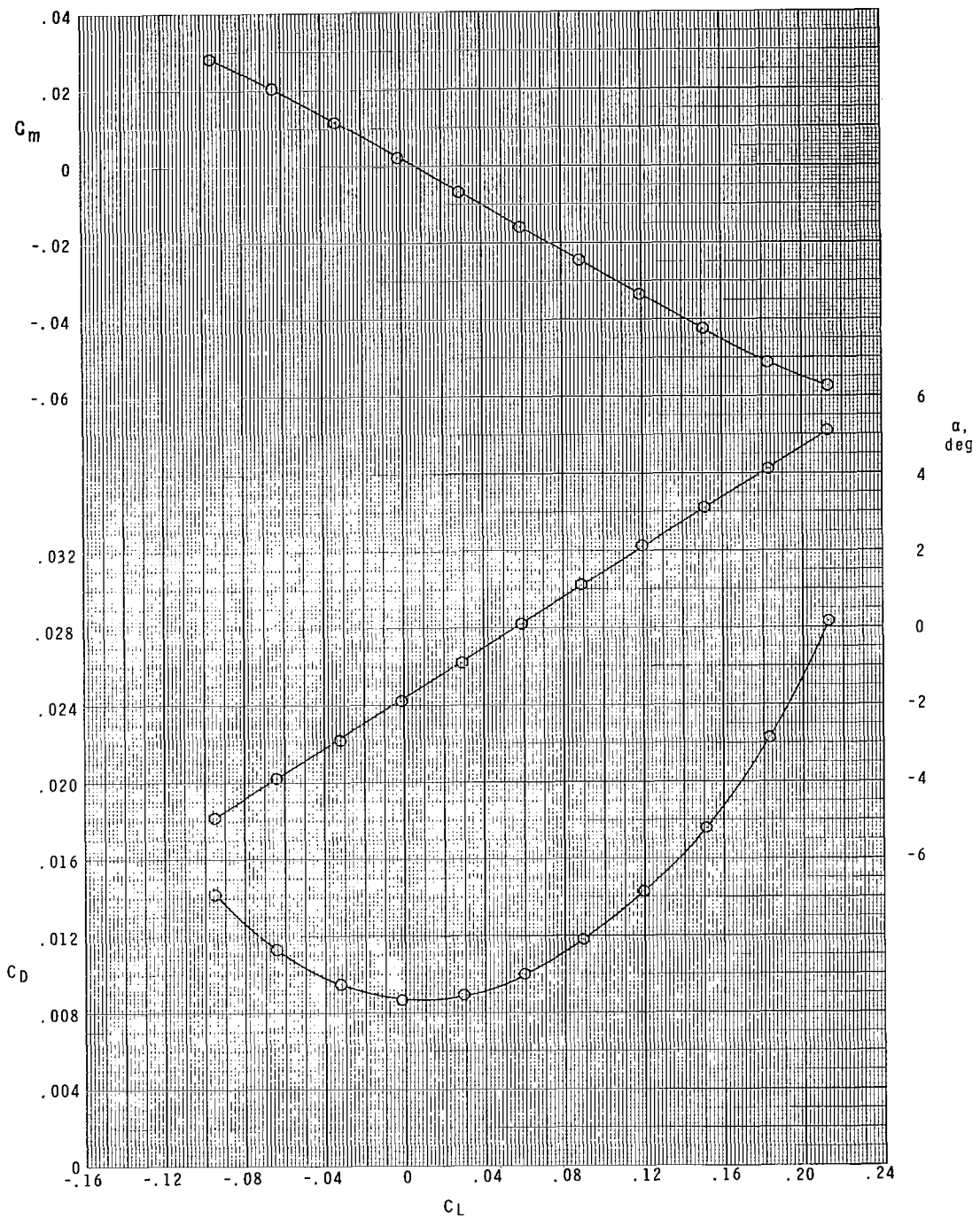
(b) Wing 2.

Figure 3.- Continued.



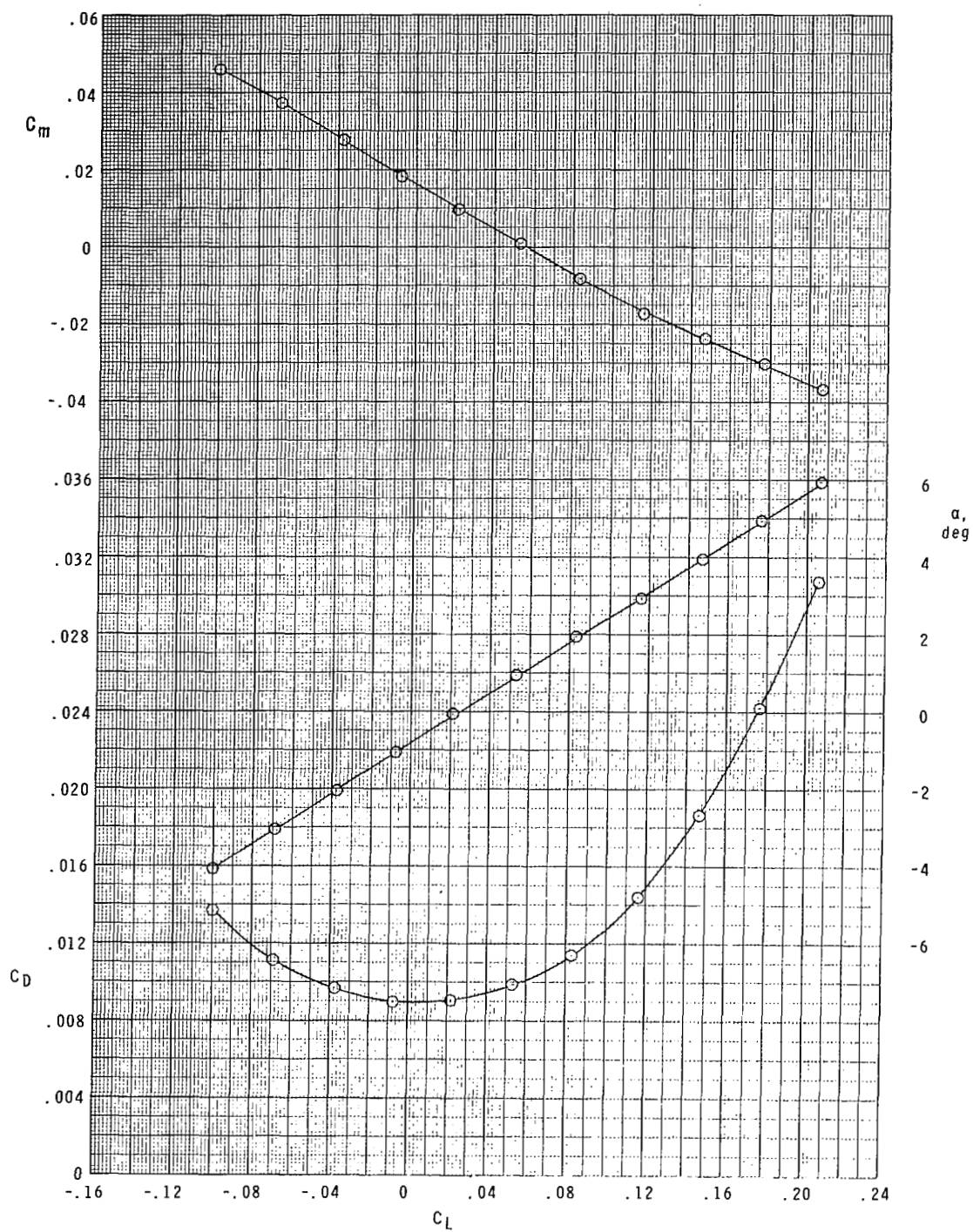
(c) Wing 3.

Figure 3.- Continued.



(d) Wing 4.

Figure 3.- Continued.



(e) Wing 5.

Figure 3.- Concluded.

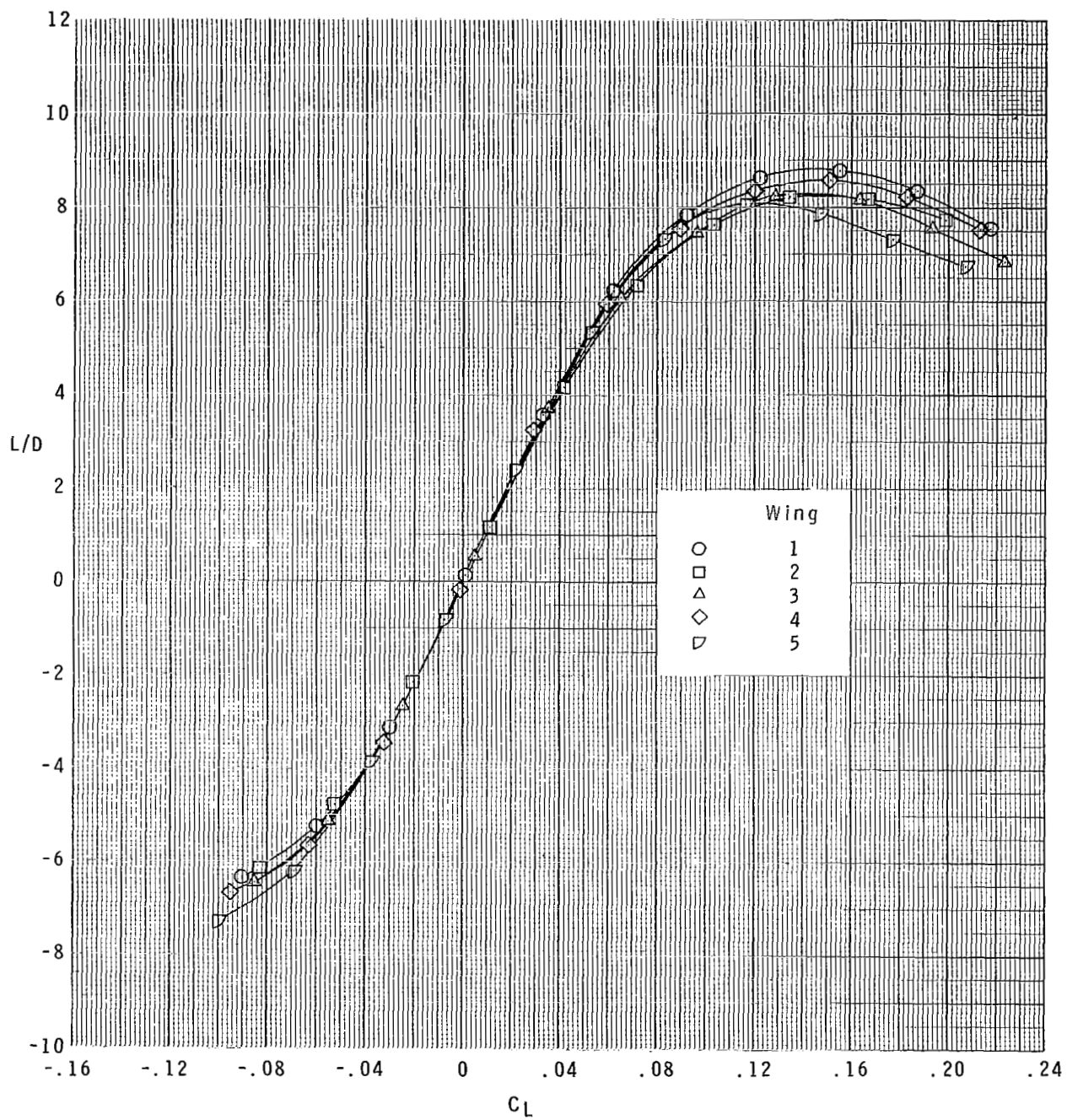


Figure 4.- Variation of lift-drag ratio with lift coefficient.

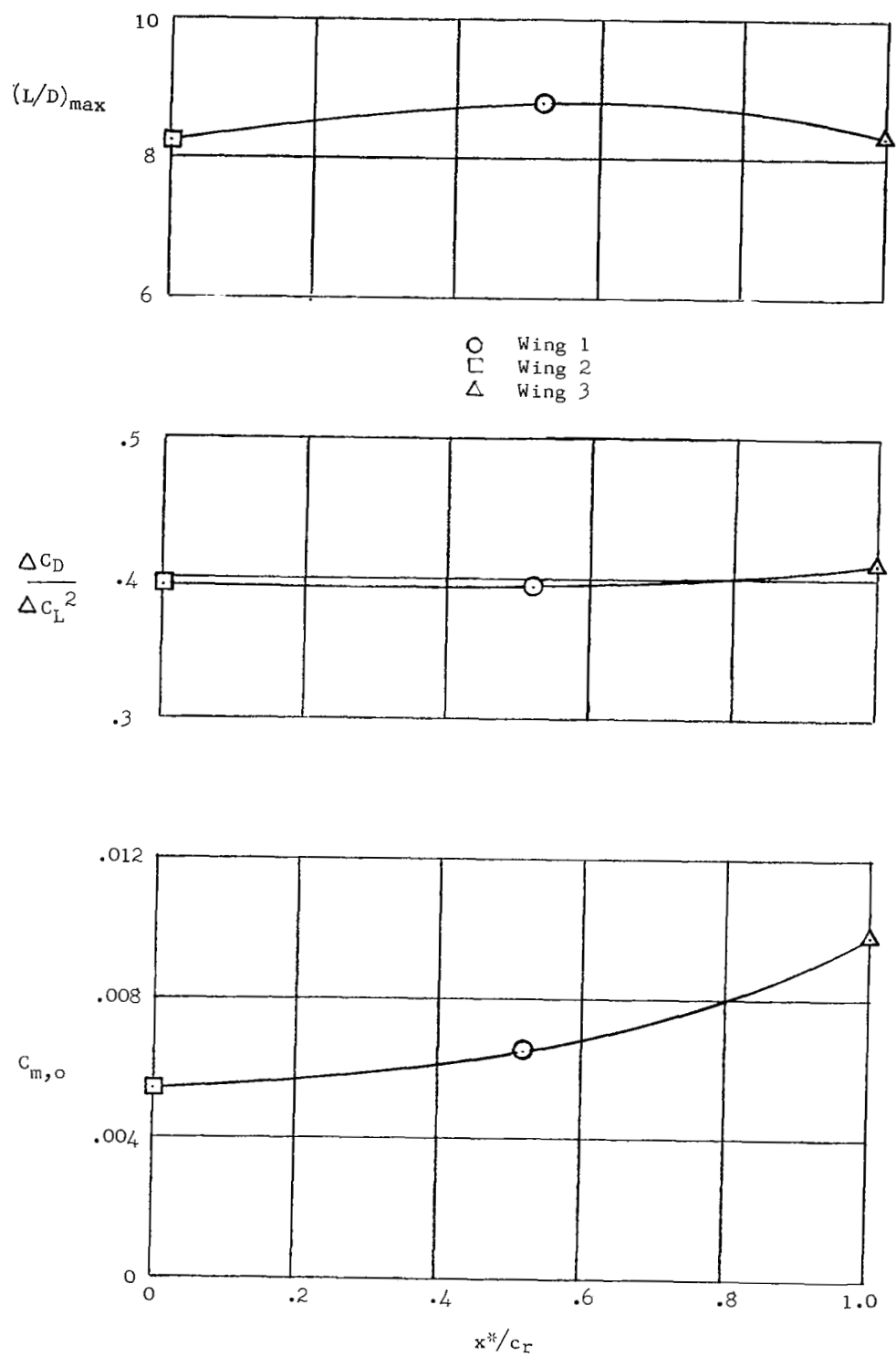


Figure 5.- Effects of shear.

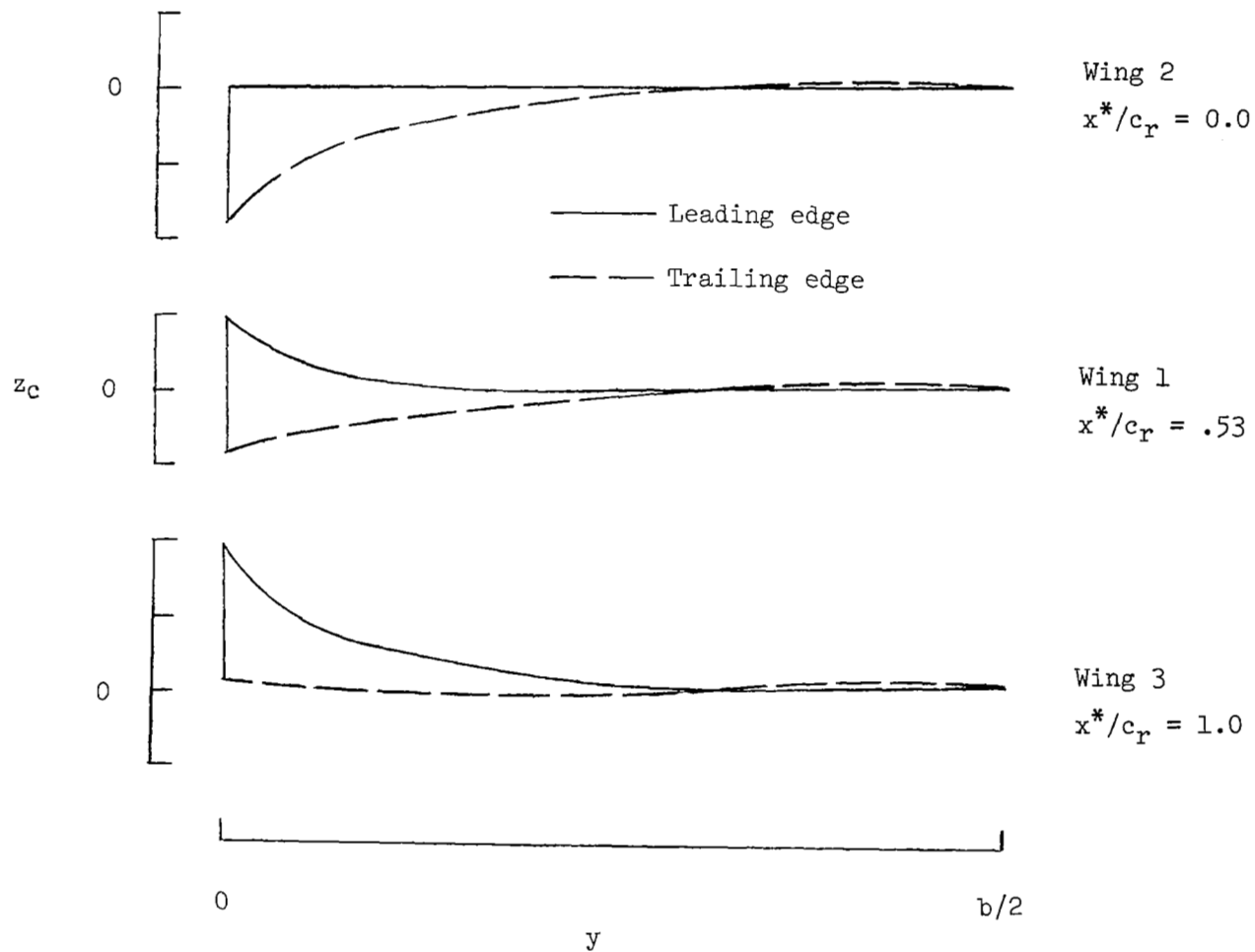


Figure 6.- Leading- and trailing-edge contours for wings 1, 2, and 3.

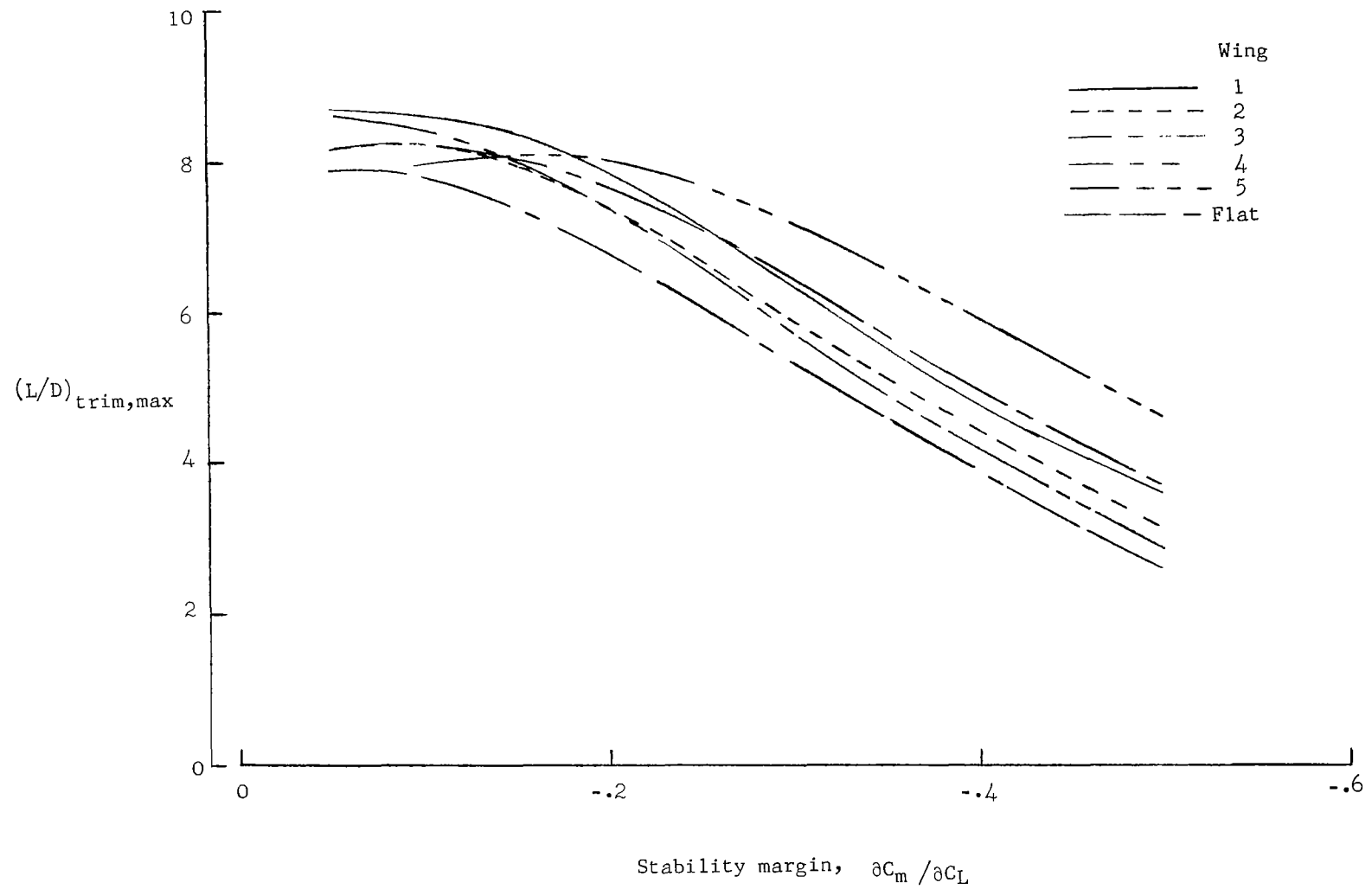


Figure 7.- Trim characteristics.